BBAA VI International Colloquium on:
Bluff Bodies Aerodynamics & Applications
Milano, Italy, July, 20–24 2008

CROSS-COMPARISON OF MEASUREMENT TECHNIQUES FOR THE DETERMINATION OF TRAIN-INDUCED AERODYNAMIC LOADS ON THE TRACKBED

Peter Deeg[⋆], Mattias Jönsson[‡], Hans-Jakob Kaltenbach[⋆], Martin Schober[∀] and Marco Weise[∀]

[⋆]Deutsche Bahn AG, DB Systemtechnik, Aerodynamics and Air conditioning
Völckerstraße 5, 80939 München, Germany
e-mail: *peter.deeg@bahn.de*, *hans-jakob.kaltenbach@bahn.de*

[‡] Deutsches Zentrum für Luft- und Raumfahrt, AS-TS, Bunsenstraße10, 37073 Göttingen, Germany
e-mail: *mattias.joensson@dlr.de*

[∀] Bombardier Transportation MLN/TSSA, Am Rathenaupark, 16761 Hennigsdorf, Germany
e-mail: *martin.schober@de.transport.bombardier.com*, *marco.weise@de.transport.bombardier.com*

Keywords: Track-side measurement, ultra-sonic anemometer, pressure probes, phase average, aerodynamic load on trackbed

Abstract: *Within the research cooperation "Aerodynamics in Open Air" (AOA) - as part of the French-German DEUFRAKO programme - a track-side measurement campaign has been carried out in Italy focusing on the loads imposed by passing trains on the trackbed. The test site on the high-speed line Roma/Firenze included both segments of ballasted track and slab track. The time series recorded from the passage of about 30 regular trains per track of the ETR 500 family have been postprocessed according to a general approach which is proprosed as a standard for future campaigns. Several types of averages, including ensemble mean, "train" average, and phase averaging have been computed and analyzed.*

It has been demonstrated that classical pressure probes as well as high-frequency ultra-sonic anemometers are suitable devices for the assessment of the average air speed above the trackbed. However, care has to be taken if details in the nose region of the leading vehicle come in to focus where local flow reversal occurs. Pressure probe signals are spoiled by the occurrence of resonances in the tubing. Low-pass filtering is a suitable way to arrive at physically meaningful signals. Fluctuations up to a frequency of $100Hz$ *could be resolved, allowing to distinguish coherent and stochastic contributions. With respect to the mean axial flow speed different probe types deviate by up to 5%.*

1 INTRODUCTION

Recently, the interest in a deeper understanding of underfloor aerodynamics of high-speed trains has increased due to the occurrence of several ballast projection incidents in European countries and Korea [5, 9, 7, 8]. Despite the fact that not all factors contributing to the phenomenon have been identified ranging from infrastructure aspects to the role of excitation of the trackbed during train passage up to differences in the underbelly design of vehicles it is well understood that the aerodynamic load imposed on the trackbed is one of the key factors. Within the context of geophysics and building aerodynamics the friction velocity $u_\tau = (\tau_W/\rho)^{0.5}$ has been identified as the critical parameter for the onset of particle dislodgement from a gravel bed subject to a tangential air stream [4, 2]. Since the wall shear stress τ_W is difficult to measure - especially on a rough surface where it is only defined in an average sense as the mean tangential force per projected surface area - it is desirable to identify other relevant flow parameters.

The ability to quantify the aerodynamic load imposed by a passing train is useful in order to assess the efficiency of countermeasures against ballast projection on existing trains [6] and as a basis for specifications for future trains and for standardizations of vehicles and infrastructure.

The measurement of the air speed near the trackbed poses many challenges that are not present in the laboratory. The probes and the data acquisition equipment must be robust due to disturbances from the presence of ground vibrations, of dust, and of strong electromagnetic fields. In addition, the equipment must be operated in an automated way and the necessity of frequent calibrations such as for hotwire probes is undesirable.

Thus, most often pressure based techniques have been used. In [5] a vertical and a horizontal rake of Pitot (Kiel) probes was used to measure air speed over a ballasted trackbed for trains passing with about $280\,km/h$. Mean axial speeds were defined as time-average between the time when the flow has reached a fully-developed state - usually between the second or third coach - and the passing of the last axle. Variations of this mean with distance from trackbed and with respect to the lateral position are shown.

Both a Pitot rake and hot-film probes were used in [3] in a trackside campaign and the vertical variation of the mean axial speed under the train is shown.

This paper reports on the outcome of a trackside measurement campaign carried out as part of the DEUFRAKO research cooperation *Aerodynamics in Open Air* in the spring of 2006 on the high-speed line connecting Florence and Rome. The site was located close to the Terranuova Le Ville tunnel and incorporated segments of ballasted track and of slab track. The study served several goals, namely to find out

- what fundamental quantities such as static pressure, air speed, and wall stress could be measured under a passing train and what accuracy respectively temporal/spatial resolution could be achieved with different techniques,
- what statistical measures (types of averages) could be derived to assess the flow field,
- how the flow evolves along the train and whether an asymptotic state develops,
- to what degree the flow varies in the lateral and vertical direction under the train, and
- how the ground roughness affects the flow and how quickly the flow adapts to a sudden change in roughness at the interface from ballasted to slab track.

The paper is organized in the following way: in section 2 the test site and the measurement devices are described. Section 3 introduces a general postprocessing method and defines different types of averages that have been used. Finally, the results from different probes are described and compared in section 4.

2 SET-UP OF THE TEST CAMPAIGN

2.1 Test site

Test teams of Deutsche Bahn, of Bombardier, and of DLR (as a subcontractor of Bombardier) installed various probes on the two tracks of the high-speed line Roma-Firenze close to the northern portal of the Terranuova-Le Ville tunnel. The site incorporated segments of ballasted track and a rail bed made out of slab track, see Fig.1.

Figure 1: Track bed at the test site including slab track and ballasted track. Note the tunnel portal and the lateral wall along the left track.

The fact that the site is located close to a tunnel might have some yet unknown implications since the boundary layer along the train will be different on both tracks - independent of the differences in the trackbed roughness itself. Similarly, the existence of a fence along the track towards Rome might affect the underfloor flow too and therefore care has to be taken when trying to generalize the results.

A total of 114 trains passing by were registered by DB on both tracks during the three days on which measurements were taken. No dedicated test runs were carried out, rather, the regularly operating trains on this line were used as test objects. Data assessment focused on a sample of approximately 30 passings (on each track) of ETR 500 train sets.

2.2 Probes

Figs. 2 and 3 show the different types of probe installations in the trackbed. Sensors included vertical and horizontal rakes of Pitot and Prandtl tubes, static pressure bores, three fast ultrasonic two-component anemometers (USA) with a sampling rate of $250\,Hz$, three Preston tubes on a metal plate, a few hot-wires, accelerometers and a special probe for measuring the forces on a small cube. The resonance frequency of the various pressure probes was determined to fall in the range from $200\,Hz$ to $360\,Hz$.

Fig. 4 shows the exact location of different probes. Most measurements took place on the track towards Florence, i.e. for trains leaving the tunnel. Bombardiers and DLRs sensor platforms were installed on slab track only whereas DB measured with identical rakes both on ballasted track and slab track (on the line towards Florence). In addition, some pressure probes were installed on the opposite track (entering the tunnel and running towards Rome) in $6\,m$ and $12\,m$ distance from the sharp interface between segments of ballasted track and slab track. Table 1 shows the numbering system used to denote the probes. The coordinates of the probes

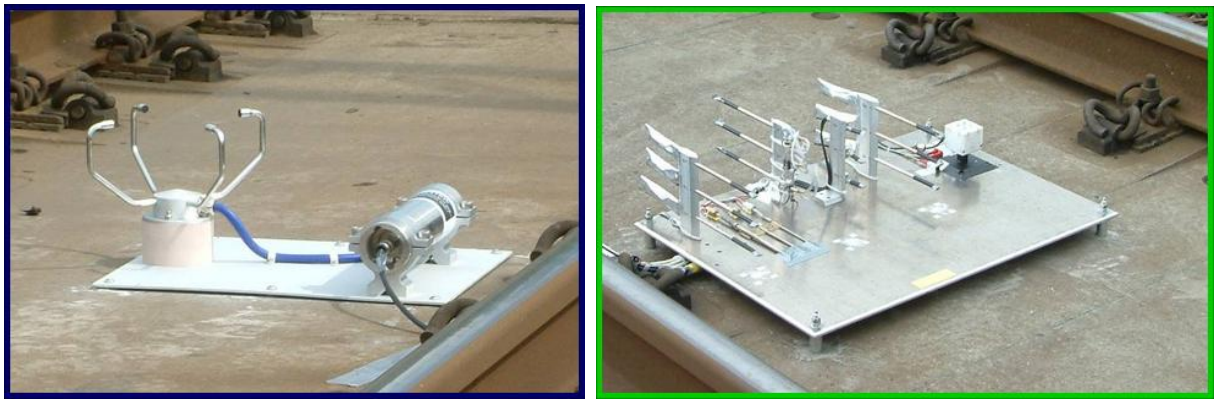

Figure 2: Left: Bombardiers ultra sonic anemometer on slab track. Right: DLRs platform with Prandtl and Preston tubes, hot wires, and devices for the measurement of forces and accelerations.

Figure 3: DBs Rakes of Pitot tubes installed on ballasted track and on slab track. The lower left shows the installations downstream of the interface between ballasted track and slab track.

are given with respect to the two systems (for each track) specified in Fig. 4. In the remainder of this paper we focus on the outcome of pressure probes and the USAs and do not report on the results from hot-wires and force measurements.

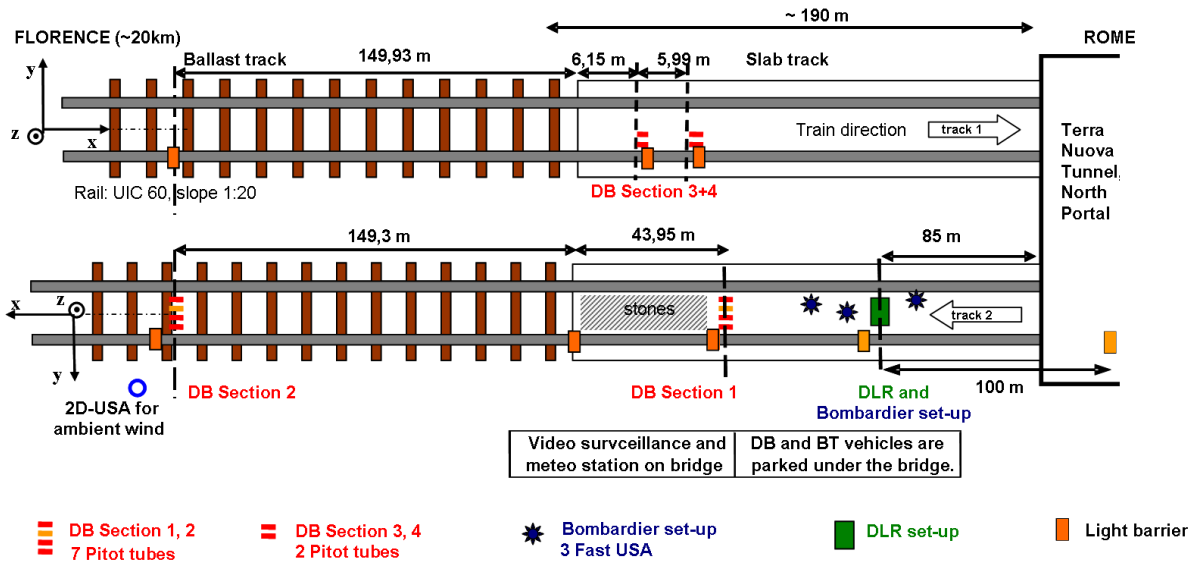

Figure 4: Test site with location of different probes.

Table 1: Lateral and vertical probe positions. The origin of the vertical coordinate is top of rail (T.O.R) and for the lateral coordinate in the center of track.

probe	track	surface	$y\,[mm]$	$z\,[mm]$
USA 1, 2, 3	Firenze	slab track	-400, 0, -200	-10
Prandtl rake 1	Firenze	slab track	0	-20, -70, -120
Prandtl rake 2	Firenze	slab track	-200	-20, -70, -120
Prandtl rake 3	Firenze	slab track	-400	-20, -70, -120
Pitot rake 1y1	Firenze	slab track	-400, -200, 200,400	-20
Pitot rake 12z	Firenze	slab track	-200	-20, -57, -94, -131
Pitot rake 2y1	Firenze	ballast	-400, -200, 200, 400	-20
Pitot rake 22z	Firenze	ballast	-200	-20, -57, -94, -131
Pitot rake 3y1	Roma	slab (6 m behind ballast)	-400, -200	-20
Pitot rake 4y1	Roma	slab (12 m behind ballast)	-400, -200	-20

3 EVALUATION PROCEDURE

3.1 Generalized data treatment

A standardized data export procedure and data format were developed within the AOA project for probes mounted in the track. The data recorded from different sensor types with different measuring rates is treated in a standardized manner in order to obtain a common data format for the later data processing. The standardized data export procedure that is described in detail in the Annex of [1]is suggested by Deutsche Bahn AG and Bombardier for all further aerodynamic measurements in the track. It shall satisfy the following criteria:

1. Supply a data set of the sensors in the track for each train passing and data on the surrounding conditions.

2. Supply a data set in a standardized format for a common post processing method independent of the sensor type used.

3. Supply air speed c_u and static pressure c_p normalized by train speed and density, taking the acceleration of the train during passing into account. For indirect measurements, allow recalculation to measured quantity (e.g. pressure of Prandtl tube).

4. Supply a well defined format for data tables of $c_u(x)$ and $c_p(x)$ over x-dimension. By definition, $x = 0$ is the first axle of the train over the sensor. A constant step size Δx and a fixed interval $-20\,m$, $500\,m$ ensures the uniform x-wise positions needed for computation of ensemble and phase averages.

5. Supply data at a rate close to the original sampling rate of the sensor to preserve sensor characteristics and to minimize effects of resampling (deletion or doubling of single values).

6. Supply additional information on the set up, the uncertainty and preprocessing (e.g. filter).

Measurements were recorded from regularly passing trains which differed considerably with respect to the train speed. Thus, ensemble averages have to be built for non-dimensional coefficients such as c_u and c_p assuming Reynolds number independence of the flow field. Although, it is assumed that environmental conditions, e.g. ambient wind speed, were similar for all runs. Between 30 and 35 passages of trains of the ETR 500 series in the speed range $190\,km/h < u_{train} < 250\,km/h$ were selected for the computation of ensemble and other averages.

3.2 Definition of averages

The standard reference speed used for normalization of velocity and pressure recordings is the local train speed $u_{train}(x)$ which might vary slightly with position x along the train in case it is accelerating or braking during passage of the sensor. Thus, dimensionless velocities and pressures are defined as

$$c_u(x) = \frac{u(x)}{u_{train}(x)} \quad \text{and} \quad c_p(x) = \frac{p(x) - p_0}{0.5\,\rho\,u_{tr}^2(x)} \quad , \tag{1}$$

where p_0 denotes ambient pressure.

We assume that a signal $c(x)$ has been measured n times with respect to the axial coordinate x with the origin referring to a well-defined position under the train. Here, n denotes the ensemble size in the sense of independent measurements. Depending on the sampling frequency, the train speed, and other constraints the signal $c(x)$ will be obtained at discrete locations x_k. The ensemble can consist of individual runs recorded by a single probe or by the recordings of several probes which are axially separated by several meters and which are placed at the same lateral and vertical positions with respect to TOR and center of track. From this set of raw data we can obtain several types of averages:

(i) Ensemble average:

$$\overline{c}(x_k) = \frac{1}{n}\sum_{i=1}^{n} c_i(x_k), \quad \overline{c^2}(x_k) = \frac{1}{n}\sum_{i=1}^{n} c_i^2(x_k), \quad \sigma(x_k) = \sqrt{\overline{c^2} - \overline{c}^2} \quad . \tag{2}$$

Here, the index i refers to the i-th passage. The r.m.s. or standard deviation σ is a measure for the local flow variation (at a given x-position) due to the stochastic character of the measured signal.

(ii) Train (or coach) average:
Often, measurements collected near the trackbed indicate that the flow reaches some sort of asymptotic state once the train head (and 1 or 2 coaches) have passed. This flow can be characterized by an average obtained from integration along a certain stretch of the train passage, say from x_1 to x_2. It can be evaluated for a single passage but usually one would combine it with the previously defined ensemble average. Since data are available at a discrete set of time instants t_k, respectively axial positions x_k, the integration is replaced by summation over $m_s = (x_2 - x_1)/\Delta x + 1 = m_2 - m_1 + 1$ consecutive samples. In the following $c_{i,k}$ denotes the measurement from passage i at position x_k. Train averages are then defined as

$$\langle c \rangle = \frac{1}{n \cdot m_S} \sum_{i=1}^{n} \sum_{k=m_1}^{m_2} c_{i,k} \quad , \quad \langle c^2 \rangle = \frac{1}{n \cdot m_S} \sum_{i=1}^{n} \sum_{k=m_1}^{m_2} c_{i,k}^2 \quad , \quad \sigma^{train} = \sqrt{\langle c^2 \rangle - \langle c \rangle^2} \quad . \tag{3}$$

Here, the standard-deviation σ^{train} denoted as "train-rms" is a measure of the "total" intensity of the fluctuating flow field. Depending on the type of train the integration (summation) bounds x_1 and x_2 (respectively m_2 and m_1) have to be chosen in a suitable way. The first-to-last axle mean falls into this category of averages.

(iii) Phase average:
If a signal exhibits some sort of regularity, e.g. a periodic behavior caused by an external or local forcing or by the boundary conditions, it can be useful, to decompose the signal in three fractions, namely the "mean", the "coherent" part, and the "stochastic" part. In an approximate sense this might be the case for a certain part of the train passage, since the Couette-type flow is interrupted in regular intervals by the presence of bogies and cross-sectional changes at the intercar connections.

Let's assume that the coaches are numbered from 1 to j_{last} and that the signal has been sampled at equidistant positions with a spacing $\Delta_x = L_c/n_c$ corresponding to an integer fraction of the length L_c of a single coach. Then the phase average involving the flow under the coaches j_1 to j_2 is defined at the positions $\widetilde{x}_k = \Delta x(k-1)$ with $k \in \{1, 2, ..., n_c\}$ and $j_c = (j_2 - j_1 + 1)$ according to

$$\overline{\widetilde{c}}(\widetilde{x}_k) = \frac{1}{n\, j_c} \sum_{i=1}^{n} \sum_{j=j_1}^{j_2} c_{i,k+(j-1)n_c} \, , \, \overline{\overline{c^2}}(\widetilde{x}_k) = \frac{1}{n\, j_c} \sum_{i=1}^{n} \sum_{j=j_1}^{j_2} c_{i,k+(j-1)n_c}^2 \, , \, \overline{\overline{\sigma}} = \sqrt{\overline{\overline{c^2}} - \overline{\overline{c}}^2} \, . \tag{4}$$

Thus, compared to the ensemble average the total number of samples has been increased by the factor j_c , i.e. the number of coaches included in this average. Note that for this type of averaging it is not necessary to consider consecutive coaches. For example for trains such as the ICE 3 one could limit the sample to those coaches with the same orientation of motor and trailer bogies. Here, the resulting standard deviation $\overline{\overline{\sigma}}$ is a measure of the intensity of stochastic fluctuations in the signal as a function of position under the coach. Now, considering the equality

$$\langle c \rangle = \frac{1}{n_c} \sum_{k=1}^{n_c} \overline{\overline{c}}_k \quad \text{and the definition} \quad \widetilde{c}_k = \overline{\overline{c}}_k - \langle c \rangle \tag{5}$$

the triple decomposition of the instantaneous signal reads

$$c_{i,k} = \langle c \rangle + \widetilde{c}_{mod(k,n_c)} + c'_{i,k} \quad . \tag{6}$$

Measures of the intensity of the coherent motion - respectively the average flow variation due to the passage of bogies and intercar gaps - and of the stochastic fluctuations are

$$\sigma^{coh} = \sqrt{\frac{1}{n_c}\sum_{k=1}^{n_c}\tilde{c}_k^2} \qquad \text{and} \qquad \sigma^{stoch} = \sqrt{\frac{1}{n \cdot m_S}\sum_{i=1}^{n}\sum_{k=m_1}^{m_2} c_{i,k}'^2} \quad . \tag{7}$$

4 RESULTS

4.1 Instantaneous signals, effect of low-pass filtering

Fig. 5 shows the recording of the ultra-sonic anemometer from one train passing. The turbulent nature of the velocity signals is evident although it should be kept in mind that the device does not measure instantaneous, pointwise velocities due to the considerable size ($\Delta x = \Delta y = 141\,mm$) of the measuring volume. When the USA signal is low-pass filtered in the same way as the pressure probes - see below - using a two-pass Butterworth multipole filter with a cut-off frequency of $75\,Hz$ it remains almost unchanged. This demonstrates that this device is in fact recording a filtered velocity signal as a result of the spatial averaging over a distance of $200\,mm$ between two sensor heads.

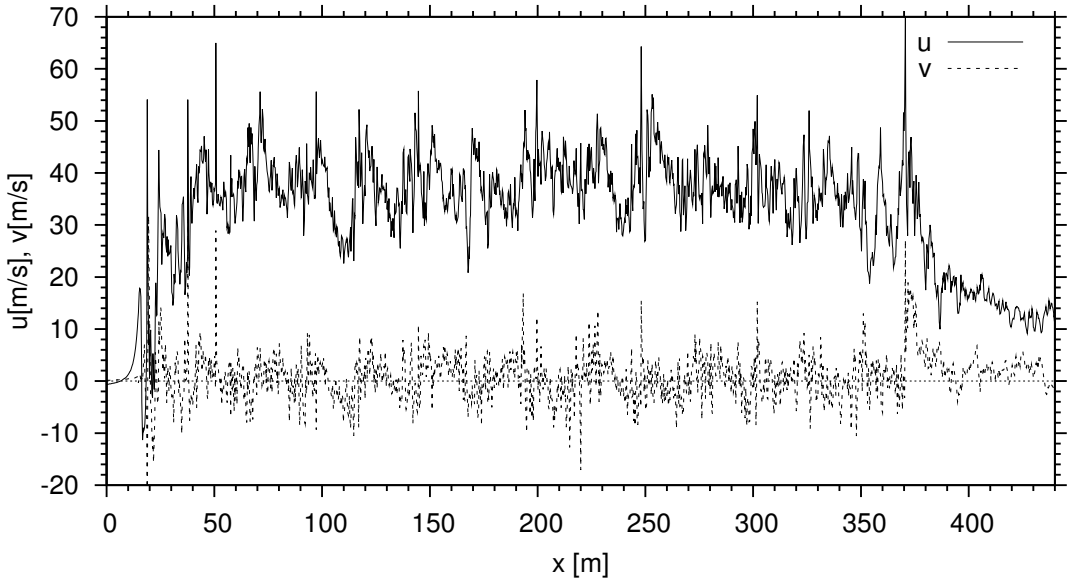

Figure 5: Time series of axial and lateral velocity component recorded with a fast USA at $10\,mm$ below top of rail.

The axial flow speed quickly rises to an average level around which it fluctuates. Lateral fluctuations are nearly as intense as the axial fluctuations. During the nose passage an intense gust of magnitude $10\,m/s$ with sign reversal occurs.

This flow reversal can not be captured correctly by the pressure probes pointing against the trains running direction. This can be seen in the instantaneous signals that are shown in Fig. 6 prior and after low-pass filtering.

It is evident that the pressure signals are spoiled by spurious oscillations. Due to different resonance eigenfrequencies and damping coefficients the pressure probes behave differently. Whereas the Pitot tubes used by DB frequently predict unphysical negative values the DLR Prandtl probe readings stay positive.

Two methods have been found to be very effective in the removal of unwanted "noise" from the signal. Use of a $75\,Hz$-low-pass filter eliminates all spurious oscillations from the instantaneous signal. Alternately, one can form ensemble or phase averages from the static and total

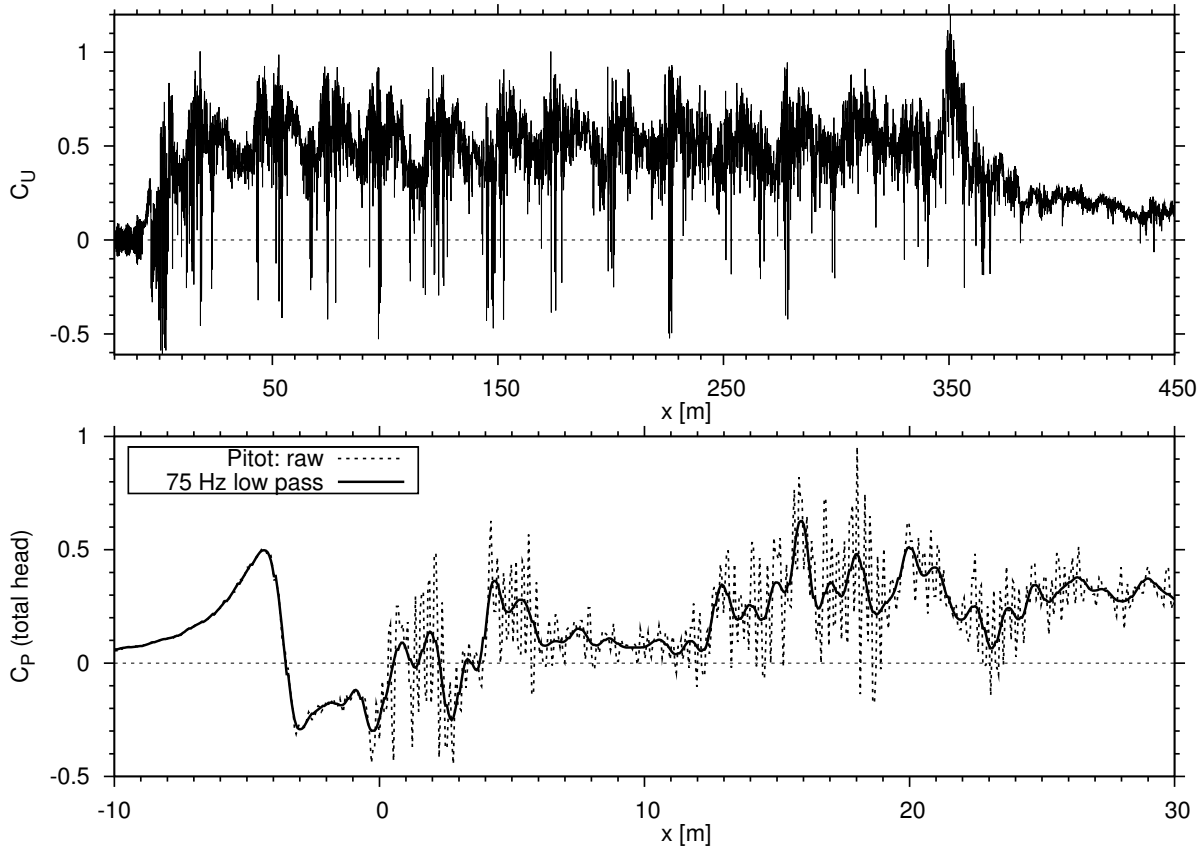

Figure 6: Instantaneous value of $c_u(x) = (c_{p,tot}(x) - c_{p,stat}(x))^{0.5} sign(c_{p,tot} - c_{p,stat})$ measured by the Pitot tube 141 at $y = -400\,mm, z = -10\,mm$ (top) and instantaneous signals of the total pressure $c_{p,tot}(x)$ without and with a low-pass filter (bottom).

pressure recordings, respectively c_p, first and derive the average flow speed afterwards as

$$\overline{c}_u^{corr} = \sqrt{\overline{c}_{p,tot} - \overline{c}_{p,stat}} \sqrt{\frac{1}{1 + T_{rms}^2}} \tag{8}$$

with a correction based on estimation of the turbulence intensity $T_{rms} = \overline{u_i' u_i'}^{0.5} / \overline{U}$.

4.2 Ensemble and phase averages

In Fig. 7 ensemble averages are compared for three probe types at almost the same vertical and lateral position. Except for the flow reversal in the nose region the three probes predict very similar ensemble averages: the flow approaches an asymptotic state with a regular pattern in the flow variation from coach to coach. Also, a similar magnitude for the peak value at the trains tail is predicted.

The development of such a regular pattern allows further comparison on the level of phase averages that are defined in the region $49.75\,m < x < 309.25\,m$ - starting from the second axle of the second coach - over 10 consecutive coaches. Fig. 8 shows examples of such averages.

Downstream of the first bogie of each coach the axial speed decays continuously since the turbulence generated in the bogie region is expected to become weaker under the smooth car body. As the second bogie and the intercar gap are reached, the near-wall flow gains momentum as a consequence of increased turbulence generation through the disturbance and constriction imposed by the bogie and the changes in cross section. The peak-to-peak variation in $\overline{\overline{c}}_u$ over

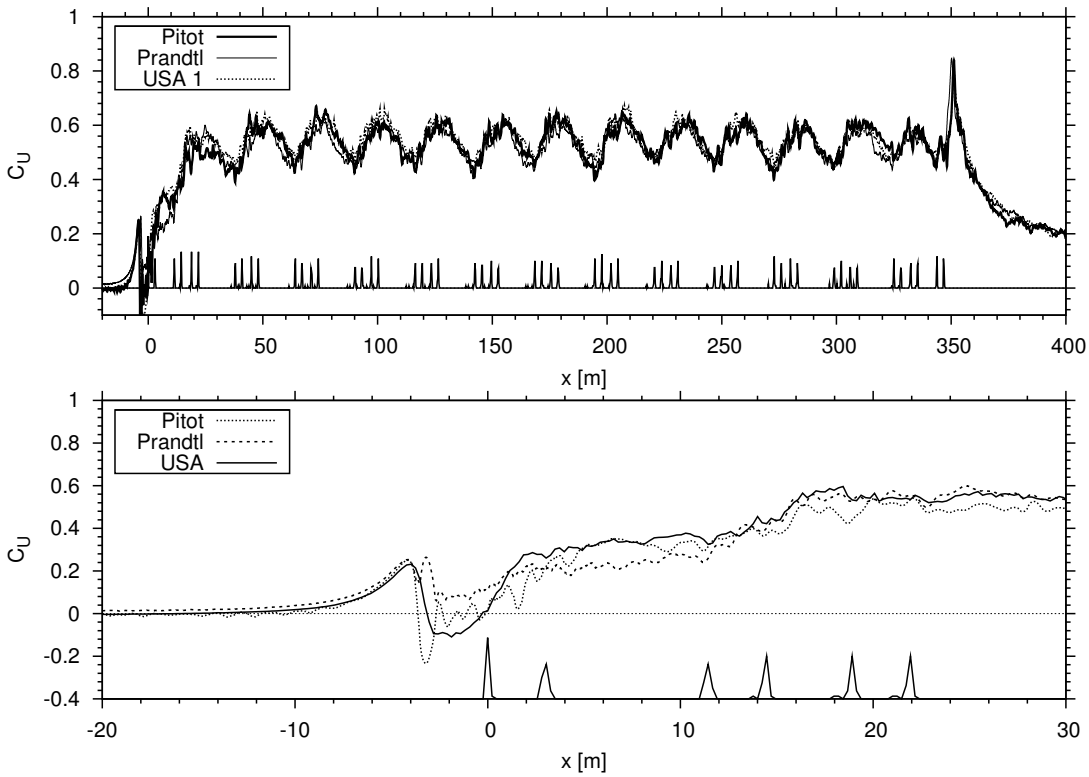

Figure 7: Ensemble average $\overline{c}_u$ from three different probes at $y = -400\,mm$ and $z = -10\,(-20)\,mm$ for the full train (top) and for the train head (bottom). Along the bottom of the diagram the average light gate signal is plotted which yields the position of wheels, allowing to identify coaches.

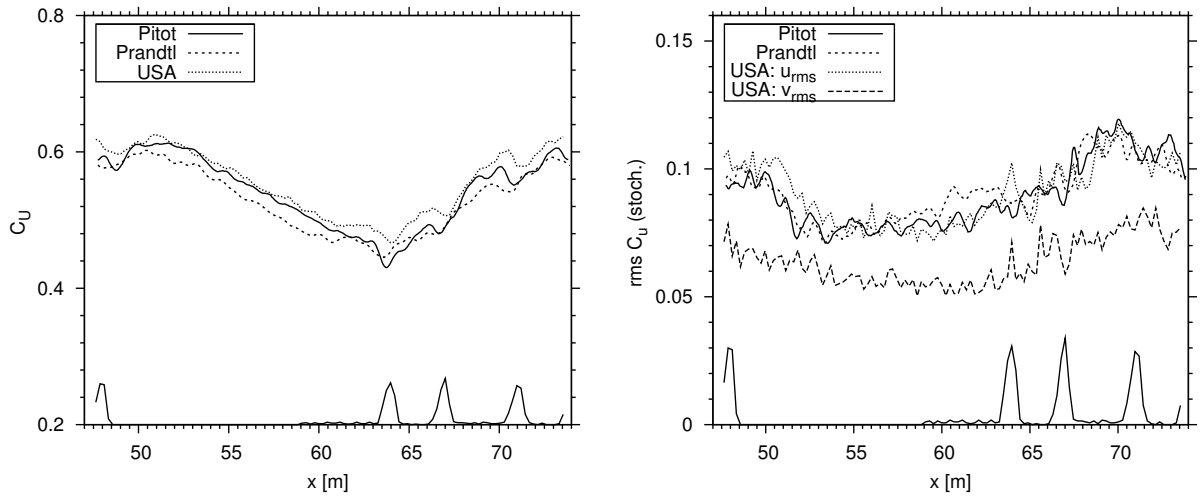

Figure 8: Phase average $\overline{\overline{c}}_u$ of axial speed (left) and of the stochastic turbulence intensities $\overline{\overline{\sigma}}_u, \overline{\overline{\sigma}}_v$ for three probe types at $y = -400\,mm$ and $z = -10\,(-20)\,mm$. Along the bottom of the diagram the average light gate signal is plotted which yields the position of the wheels. $x = 48\,m$ corresponds to the second axle of the first bogie of a coach. The center of the intercar gap is located at $x = 68.5\,m$.

the entire "cycle" amounts to about 40% of the average over the entire coach.

Fig. 8 (right) shows how the intensity of the stochastic fluctuations varies along a coach. The gradual decay of the turbulence intensity downstream of the first bogie becomes evident as well as the continuous increase from the first axle of the second bogie of a coach until the second axis of the first bogie of the next coach is reached. Over the entire length of the coach the

agreement between results obtained from different probes is very good. At the central position ($y = 0\,mm$) the peak-to-peak variation is largest with the maximum of $\overline{\overline{\sigma}}_u$ being 70% larger than the minimum near $x = 60\,m$. The USA measurements show that the ratio of axial to lateral turbulence intensity is not constant along the coach. It can be regarded as a measure of the degree of anisotropy of the turbulent fluctuations.

Fig. 8 (left) shows that the main difference in the curves measured by different probes consists in an approximately constant offset in $\overline{\overline{c}}_u$. Thus, it is justified to base a quantitative comparison of different devices on the average $\langle c_u \rangle$ over the train in the range $47.75\,m < x < 309.25\,m$. Since the "train average" was determined exactly over the same spatial range as the phase average, namely 10 consecutive coaches, it is identical to the "coach average", i.e. the mean of the phase average over the length of a coach.

Table 2 summarizes the results for the train average $\langle c_u \rangle$ and the r.m.s. of coherent and stochastic fluctuations. The coherent r.m.s. can be regarded as a measure of the average deviation of the phase average from the coach (train) average.

Table 2: Comparison of train (or coach)-averages of axial speed and the r.m.s. of coherent and stochastic fluctuations at three lateral positions near top of rail, normalized by c_u at $y = 0\,mm$. For the pressure probes the averages are computed either from $75\,Hz$ low pass filtered pressure data or according to eq. 8 using $T_{rms} = 0$.

Lateral position y	probe	$\langle c_u \rangle$		σ_{coh}		σ_{stoch}
		low pass	eq. 8	low pass	eq. 8	low pass
$0\,mm$	USA 2	100.0 %		6.9 %		14.9 %
	Prandtl 4	97.5 %	98.5 %	6.8 %	6.9 %	14.5 %
	USA 2 /Prandtl 4	1.026	1.015	1.0089	0.9902	1.0266
$-200\,mm$	USA 3	97.5 %		8.3 %		14.7 %
	Pitot 131	95.9 %	97.0 %	8.2 %	8.3 %	14.8 %
	USA 3 /Pitot 131	1.017	1.005	1.0164	1.0050	0.9935
$-400\,mm$	USA 1	94.8 %		8.2 %		15.1 %
	Prandtl 1	90.4 %	91.7 %	8.2 %	8.2 %	15.6 %
	Pitot 141	92.4 %	93.6 %	8.8 %	8,9 %	15.5 %
	USA 1/Pitot l41	1.026	1.013	0.9272	0.9177	0.9780
	USA 1/Prandtl 1	1.049	1.034	0.9947	0.9986	0.9693
	Prandtl 1/Pitot l41	0.978	0.979	0.9322	0.9190	1.0089

Table 2 demonstrates that in general the mean axial speed measured by the pressure probes is by 2-5% lower than the value of the USA if the low-pass filtered pressure probe signal is used. A comparison with $\langle c_u \rangle$ obtained from the average of the dynamic pressure according to eq. 8 yields slightly better agreement. However, this is somewhat misleading since no correction for the turbulence level was made for the values reported in Table 8, i.e. $T_{rms} = 0$ was used. With such a correction the deviation from the USA signal would be larger. It has been checked whether the deviation might be related to the fact that the USA measures an average over the distance of $141\,mm$ between transmitter and receiver using spatial gradients of the mean. However, the evidence for this is weak. If the averages are derived from unfiltered pressure probe signals the deviation increases up to 6% for the mean (at position $y = -400\,mm$).

With the exception of the Pitot tube at position $y = -400\,mm$ (σ^{coh} only) a very good agreement for the r.m.s. of coherent and stochastic fluctuations is found for all probes if the comparison is based on the low-pass filtered pressure signals. This demonstrates that both measurement techniques yield information in the same frequency range. With other words, even

the pressure probes seem to be suitable to derive some useful information on the intensity of velocity fluctuations in the low-frequency band below $100\,Hz$, thereby allowing to distinguish between coherent and stochastic components in the flow variation. The r.m.s. of the stochastic fluctuation (involving only contributions from the frequency band $0 < f < 75\,Hz$) is approximately twice as large as the r.m.s. of the coherent motion associated with the regular flow interruption by bogies and coaches.

4.3 Lateral and vertical variation

Fig. 9 (left) shows how the mean axial speed varies with lateral position. Aside from the previously discussed systematic differences between the probes a similar trend is found. The speed decreases weakly from the center towards the outer position by 5% for the USA and by 8% for the Prandtl tube. Prandtl and Pitot tube show exactly the same trend. Furthermore, the Pitot tube measurements indicate that the flow is almost symmetrical with respect to the centreline of the track.

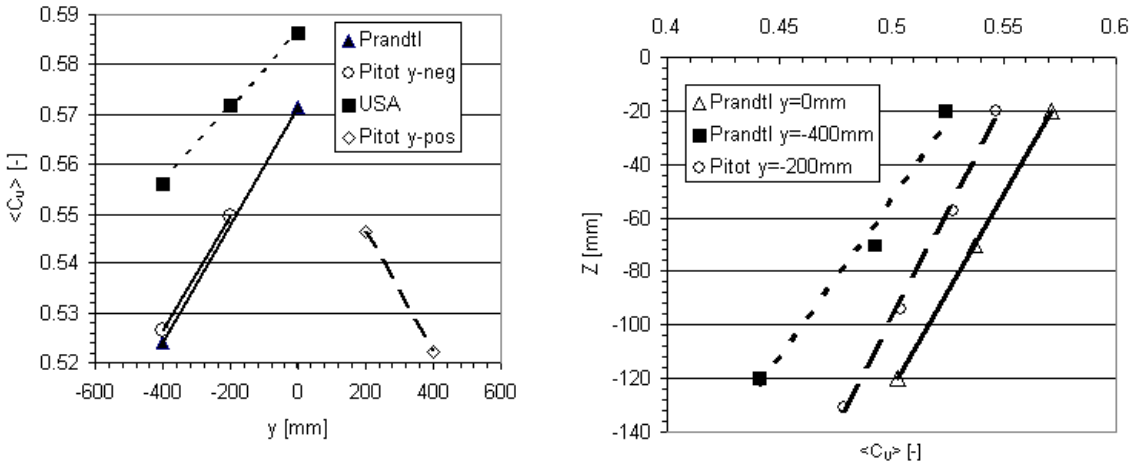

Figure 9: Left: Lateral variation of $\langle c \rangle_u$ at $z = -10\,mm$ over slab track. Right: vertical variation of $\langle c \rangle_u$ at $y = -200\,mm$ over slab track.

Fig. 9 (right) shows an almost linear relationship between the axial speed and the distance from the concrete surface. The slope of the linear fit to the measurements is about 10% higher for the lateral position $y = -200\,mm$ compared to the centreline. The vertical gradient can be used to estimate the expected difference in $\langle c \rangle_u$ from the $10\,mmm$ vertical difference in probe positions. The expected difference of $\langle c \rangle_u$ due to the vertical difference in probe position is in the order of 1 % which is too small to explain the observed differences in the order of 5 % between different probe types.

Estimates for the wall shear stress τ_w and the equivalent sand grain roughness k_s have been derived from the vertical rake measurements. Assuming the logarithmic law of the wall for a rough surface to be applicable here in the form

$$\langle c_u \rangle = m \, \ln \frac{z}{L_{ref}} + b \quad \text{we obtain} \quad \frac{u_\tau}{u_{train}} = \kappa \cdot m \quad \text{and} \quad \frac{k_s}{L_{ref}} = \exp\left(\kappa\, B - \frac{b}{m}\right) . \quad (9)$$

From the Pitot tube rake the measurements at the highest position ($z = -20\,mm$) was not considered in this evaluation. Results are given in Table 3 for the Pitot tubes for different choices

of the virtual origin. The result depends considerably on the choice of the virtual origin. The most likely value for the origin is $z_{origin} = -220\,mm$ over slab track. Both the Pitot and the Prandtl rake predict a friction velocity magnitude in the order of $c_\tau = u_\tau/u_{train} = 0.08$ for the positions $|y| \leq 200\,mm$. The fact that the Prandtl rake predicts somewhat higher values than the Pitot rake can partially be contributed to the fact that for the Prandtl rake the first off-wall position was $100\,mm$ above the concrete which is probably too far off from the wall to properly catch the log region of the mean profile. This is corroborated by the finding that the result is closer to the Prandtl tubes if the Pitot rake measurements are evaluated using measurements from the three upper vertical locations.

Table 3: Estimation of wall shear stress from vertical variation of $\langle c_u \rangle$ measured with a Pitot tube rake.

probe	z_{origin}	offset b	slope m	$c_\tau = u_\tau/u_{train}$	$k_s[mm]$
slab track (121-124)	-202	0.1873	0.1588	0.064	9.9
slab track (121-124)	-220	0.1162	0.1855	0.076	17.4
ballast (221-224)	-192	-0.2105	0.3015	0.124	65.6
ballast (221-224)	-202	-0.2933	0.3356	0.138	78.2
ballast (221-224)	-220	-0.4439	0.3962	0.162	100.0

The increase of c_τ towards the outer lateral position might be caused by the influence from the roughness associated with the fastening of the rails to the concrete. The estimate for $k_s = \mathcal{O}(10\,mm)$ of the concrete surface appears to be unrealistically high and indicates that this type of evaluation might not be applicable here. Possibly, the sensors should have been positioned closer to the ground in this case.

On the ballasted track the virtual origin it is not well defined. It is somewhat surprising that the estimate of the friction velocity on ballasted track yields only an about a factor of 2 higher value compared to slab track. On the other hand, the estimate for the equivalent roughness $k_S = \mathcal{O}(80\,mm)$ seems to be more realistic here.

The friction velocity on the ballasted surface can be used to estimate at what train speed dislodgement of particles would set in according to Bagnolds threshold for the Froude number [4]:

$$U_{critical} = \frac{u_{\tau,thresh}}{c_\tau} = \frac{1}{\widehat{A}}\sqrt{\frac{\rho_S - \rho_A}{\rho_S}\,d_p\,g} \quad . \tag{10}$$

Here, d_p denotes the average particle diameter and ρ_S and ρ_A are the densities of particles and air, respectively. It turns out that for $c_\tau = 0.14$, $d_p = 0.04\,m$, $\rho_A = 1.2\,kg/m^3$, $\widehat{A} = 0.1$, and $\rho_S = 2600\,kg/m^3$ the critical train speed according to eq. 10 is as low as $75\,km/h$. This is much lower than the speed well above $250\,km/h$ for which ballast projection was observed to occur under the ETR 500 on a trackbed where the ballast was not lowered below top of sleepers.

There are two reasons which might explain part of this discrepancy. On one hand, in the "SÜMKA" wind tunnel experiment investigating the particle dislodgement in scale 1:10 from a trackbed model [1] a lift-off was only observed for considerably higher values of the dimensionless threshold $\widehat{A}$. On the other hand, the onset of particle movement is not equivalent to the onset of noticeable ballast projection since particles have to be accelerated further by wind forces in order to reach sufficient kinetic energy to be able to be projected against the trains underbelly.

4.4 Influence of the ground conditions

An important question in the context of definition of a common measurement procedure for the assessment of the aerodynamic load imposed by a train is concerned with the effect of a change in roughness on the flow evolution under the train. In order to gain some insight into this topic results from Pitot tube measurements at three cross-sections have been compared. On the track towards Rome two Pitot tubes (331 and 341) were placed $6\,m$ downstream of the sudden change from ballasted trackbed to slab track and two others (431 and 441) at $12\,m$ distance. The measurements are compared with the values obtained by probes 131 and 141 on the opposite track, representing an infinite stretch of slab track ahead of the measurement site. Ideally, one would expect that flow properties at the $6\,m$ and at the $12\,m$ position to gradually approach the ones on the other track.

The phase average $\overline{\overline{c}}_u$ for the three positions is shown in Fig. 10. There is no trend to observe from $6\,m$ over $12\,m$ towards infinity. In contrary, the difference between the signals at the $6\,m$ and the $12\,m$ positions are much smaller than the difference between the $12\,m$ position and the reference section on the opposite track.

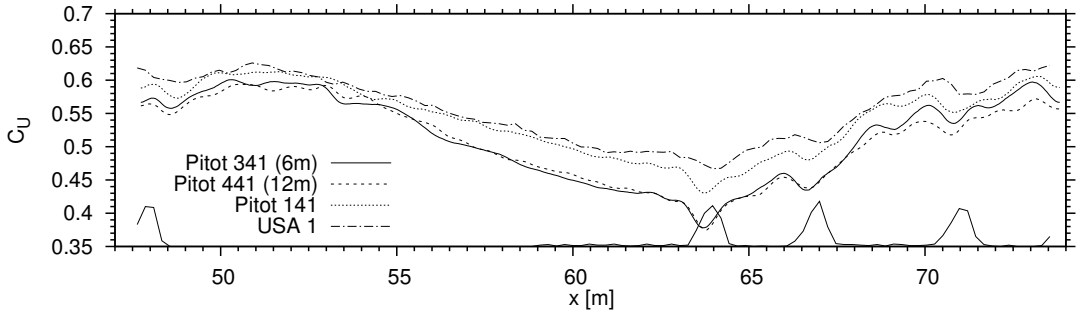

Figure 10: Phase average $\overline{\overline{c}}_u$ at $y = -400\,mm$ and $z = -10\,mm$ measured with Pitot tubes over slab track on cross sections 1,3, and 4. Along the bottom the light gate signal is plotted which indicates the positions of the wheels.

The same conclusion follows from train (coach) averages (not shown) and from the examination of stochastic and coherent contributions to the turbulence intensity. What can we deduce from this finding? There are two possible explanations. Even a $12\,m$ distance from a change in surface roughness might be too short for the flow to fully adapt to the change in boundary conditions. On the other hand we can not exclude that some unknown systematic differences exist between both tracks, such as that trains emerge from a tunnel on the Firenze track or that on the Rome track there is a vertical fence close by the track.

Possibly, the side-wall boundary layers along the train are different in both cases and this might also affect the flow evolution in the underfloor region. It appears that the data collected during this campaign are not sufficient in order to arrive at final conclusions with respect to definition of a common measurement procedure, especially if a “reference” surface shall be installed in the track on which probes shall be mounted.

4.5 Static pressure variations

Phase averages of the static pressure along the coach are shown in Fig. 11. The distinct pattern seems to be correlated with geometrical features of the train such as begin and end of the bogie cavities or passing of the axles. A weak lateral variation is observed. It is not clear whether this is a measurement uncertainty, e.g. from calibration, or whether it is real. There

is no evidence of a sustained (in the sense of train or coach average) deviation of the mean pressure from the ambient pressure.

The average static pressure signal shows that during train passage the trackbed is exposed to a moving axial pressure gradient $\partial\overline{\overline{p}}/\partial x$, respectively a ballast particle experiences a mean temporal change $\partial\overline{\overline{p}}/\partial t = \partial\overline{\overline{p}}/\partial x \cdot u_{train}$. The magnitude of these gradients - which last not longer than $1\,m$ - can be estimated from Fig. 11 to be in the order of $\partial\overline{\overline{c}}_p/\partial x = 0.3\,m^{-1}$. For a train cruising with a speed of $250\,km/h$ this corresponds to a spatial gradient of $850\,Pa/m$ respectively a temporal gradient $59\,kPa/s$ lasting over $0.0144\,s$.

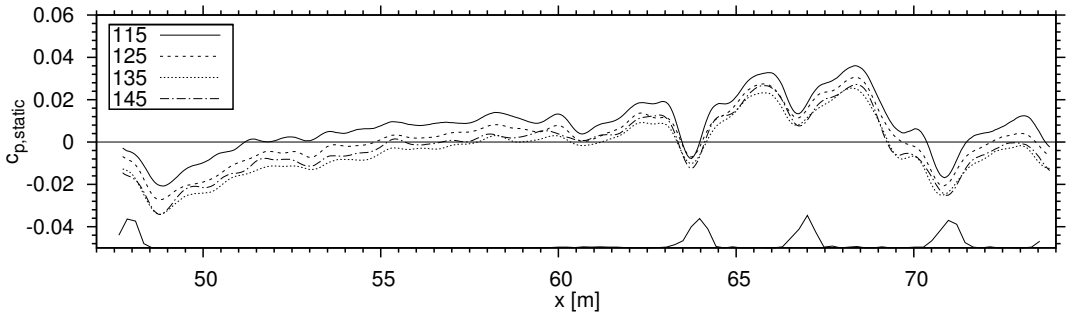

Figure 11: Phase average of static pressure at four lateral positions measured on slab track surface.

5 CONCLUSIONS

For the assessment of the air speed in the underfloor region it is useful to distinguish several types of averages, ranging from ensemble averages (at a fixed axial position), phase averages (making use of the repeating flow pattern under similar shaped coaches), and train or coach averages. This allows to separate coherent variations from stochastic fluctuations due to the turbulent nature of the flow. Measurement of the stochastic r.m.s. might be relevant for ballast projection assessment since it correlates with the friction velocity [10] which is hard to measure directly.

The fast ultra-sonic anemometer (USA) yields the most reliable raw signals (time series) among the probes tested. The signals recorded by the installed pressure probes (Pitot or Prandtl tubes) are massively spoiled by resonances in the tubing. Low-pass filtering seems to be a suitable method to eliminate these spurious oscillations from the instantaneous recordings. Alternately, averages of the velocity can be deduced from averages of the pressure difference. Pressure probes do not yield reliable signals during head passage. The short flow reversal ahead of the first axle can only be captured by the USA.

With respect to determination of mean values (averages) in the sense of phase-average, i.e. the repeating, uniform flow pattern under each coach, and intensity of coherent and stochastic contributions to the velocity fluctuations all three probes yield similar values. For the "train mean", the pressure probes used in this campaign predict lower (up to 5%) values than the USA. With respect to the coherent r.m.s. the maximum deviations between probes amount to 9%, for the stochastic part up to 3.5%. Thus, pressure probes and USA yield information in a similar frequency range (below $100\,Hz$). In this range of scales, the stochastic intensity (rms) of axial fluctuations is about twice as large as the coherent contribution.

The lateral variation of the axial flow near TOR over a spanwise distance of $400\,mm$ from the track centreline is weak (7%). A considerable vertical variation of axial flow speed occurs between trackbed and TOR. The accuracy of the estimation of the (mean) wall shear stress

from vertical rake data assuming a log-law needs to be analyzed more carefully and the vertical positions of probes might be better adapted for this purpose.

A change in roughness of the trackbed modifies the mean axial flow in accordance with common knowledge on flow along rough plates. Pitot rake measurements indicate that the friction velocity along ballasted track is at least twice as high as on the concrete surface. With respect to the length that it takes until the flow has adapted to a sudden change in the trackbed roughness no conclusions could be drawn from this study. It appears that there exist other (unknown) differences in the flow evolution on both tracks at this measurement site.

ACKNOWLEDGMENT

We thank Roberto Roberti and Luca Bocciolini from Trenitalia and Mario Testa from RFI for their dedication in organizing of the test campaign. Bombardier acknowledges the support and dedication of DLR's team headed by Sigfried Loose with respect to preparation of the sensor platform and for carrying out the measurements. Public funding under grants 19 S 5009 A and 19 S 5009 B from the German ministry of economy (BMWi) under the auspices of S. Meuresch within the French-German DEUFRAKO programme is acknowledged. The grant was monitored by A. Wurm from TÜV Rheinland Group.

REFERENCES

[1] DB AG. DEUFRAKO Project Aerodynamics in Open Air (AOA), WP 1, Underfloor Aerodynamics, Summary report. *Technical report*, Deutsche Bahn AG, DB Systemtechnik, Munich, Germany; H.-J. Kaltenbach (ed.) 132 pp., 2008.

[2] R.S. Anderson, M. Sorensen, and B.B. Willetts. A review of recent progress in our understanding of aeolian sediment transport. *Acta Mechanica [Suppl.]*, 1:1–19, 1991.

[3] A. Ido, S. Saitou, K. Nakade, and S. Iikura. Study on under-floor flow to reduce ballast flying phenomena. In *Proceedings of the 8th World Congress on Railway Research, May 18-22, 2008 in Seoul, Korea*, 2008.

[4] R. J. Kind. Tests to determine the wind-speeds for scouring and blowoff of rooftop gravel. In *Proceedings of the Fourth Intern. Conference on Wind effects on buildings and structures. Heathrow, 1975. Eds.: K. J. Eaton. Cambridge Univ. Press*, pages 591–604, 2006.

[5] H. B. Kwon and C. S. Park. An experimental study on the relationship between ballast-flying phenomenon and strong wind under high-speed train. In *Proceedings of the 7th World Congress on Railway Research,in Montreal, Canada, paper 625*, 2006.

[6] C. Müller. ICE 3: Nun auch in Frankreich. *EI- Eisenbahningenieur*, 56:82–84, 11 2005.

[7] N. N. ICE-3-Zulassung in Frankreich vor dem Abschluss. 2005.

[8] N.N. Civils and signals block speed-up on world's fastest line. *Railway Gazette International*, (04):179, 2005.

[9] F. Panier. Zulassung des ICE 3 in Frankreich - die praktische Erprobung. *EI - Eisenbahningenieur*, 56:514–517, 11 2005.

[10] H. W. Tieleman. Strong wind observations in the atmospheric surface layer. *Journal of Wind Engineering and Industrial Aerodynamics*, 96:41–77, 2008.